Linking Surface Potential and Deprotonation in Nanoporous Silica: Second Harmonic Generation and Acid/Base Titration

R. Kramer Campen,[†,‡,§] Allison K. Pymer,[†,∥] Satoshi Nihonyanagi,[†,⊥] and Eric Borguet*[,†]

Department of Chemistry, Temple University, 1901 N. 13th Street, Philadelphia, Pennsylvania 19122, and Department of Geosciences and Earth and Environmental Sciences Institute, Pennsylvania State University, University Park, Pennsylvania 16802

Received: April 26, 2010; Revised Manuscript Received: August 18, 2010

The adsorption of ions at the oxide/water interface is important for a variety of technological and environmental applications. Understanding ion adsorption is complicated, even for smooth planar surfaces, because it is the result of both chemical and electrostatic effects. Adsorption on rough or porous phases further requires description of the influence of pore geometry. In this work we systematically study ion adsorption and charge development in nanoporous silica. We do so using conventional titration techniques and a noninvasive, all optical method of measuring particle surface potential: second harmonic generation. We find that at pH greater than ≈6.5 surface proton loss is completely compensated by counterion adsorption, leading to little detectable gain in surface charge, and that surface deprotonation above this threshold pH is dominated by internal surface sites. Such a threshold pH, above which acid/base or ion titration curves of porous mineral phases are dominated by adsorption to internal surfaces and surface charge is relatively constant, is expected to be a general feature of the porous oxide/water interface and its explicit consideration important in describing the adsorption of large ions on porous mineral phases and the stability of aqueous suspensions of porous mineral particles. Our results also suggest that the surface of nanoporous silica, synthesized using the method of Stöber, does not polymerize in aqueous solution.

I. Introduction

An accurate, macroscopic description of contaminant and nutrient adsorption on mineral surfaces is essential in protecting groundwater resources and understanding the ecological consequences of climate change.[1−3] Quantitative meter to kilometer scale descriptions of these interfacial phenomena are likely to be the most generally applicable, over variable solution chemistry and temperature, if derived from an accurate molecular level description of the mineral/water interface. Additionally, such interactions have been argued to be of importance in the evolutionary origins of amino acid chiral selectivity and are of likely relevance to the design of new materials with improved biocompatibility or electronic properties.[4−6]

In environmental systems, the quest to understand contaminant and nutrient transport has driven interest in the extent to which small, soluble ions adsorb on mineral surfaces. In geological terranes that lack particulate mineral phases, this interaction determines the mobility of the adsorbing compound. In terranes that have particulate mineral phases, the adsorption of ions on colloidal surfaces often influences suspension stability and thus indirectly determines the mobility of the adsorbate.[7,8] The adsorption of ions at mineral surfaces is of particular interest, in contrast to neutral species, because it influences both surface chemistry and charge.[9]

For example, in the silica/aqueous system, adsorption of protons from solution regulates an equilibrium between positively charged (⟩$SiOH_2^+$), neutral (⟩SiOH), and negatively charged (⟩SiO^-) groups (where ⟩ indicates bonding to the underlying solid). Describing such reactions at oxide/water interfaces requires understanding how surface functional groups interact with water and adsorbate functional groups (i.e., chemical forces), how the presence of an array of charge at the mineral surface influences the ΔG_{ads} of adsorbates (i.e., electrostatic forces), and the manner in which these two factors are related.

For more than 30 years two basic experimental approaches have been used to investigate adsorption of ions at the mineral/water interface. In the first approach, adsorption is measured directly by titrating suspensions of mineral particles with an ion of interest. The resulting measured adsorption is the result of both electrostatic and chemical forces. In the second, electrostatic forces at mineral surfaces are directly probed using electrokinetic methods. A mathematical model that self-consistently reproduces both titration and surface potential data by postulating a molecular mechanism of ion adsorption would be expected to extend our understanding of these types of interactions.

In response to this need, a variety of surface complexation models (SCMs) have been developed over the past 30 years.[9,10] While the details of the SCMs differ, they share a common set of assumptions. First, ions adsorb in discrete planes and/or at spatially discrete surface sites. Second, counterions can be described as point charges and co-ions are represented implicitly. Third, the surface is planar and impenetrable to ions. The first assumption will be rigorously applicable only in the absence of atomic level defects as the surface must be uniform on the scale of individual counterions. The second

* To whom correspondence should be addressed. E-mail: eborguet@temple.edu.
† Temple University.
‡ Pennsylvania State University.
§ Now at FOM Institute of Atomic and Molecular Physics [AMOLF], Science Park 104, 1098 SG, Amsterdam, The Netherlands.
∥ Now at Department of Chemistry, Room 419 Latimer Hall, University of California, Berkeley, Berkeley, CA 94720-1460.
⊥ Now at Molecular Spectroscopy Laboratory, RIKEN (The Institute of Physical and Chemical Research), 2-1 Hirosawa, Wako 351-0198, Japan.

10.1021/jp1037574
Published on Web 10/13/2010

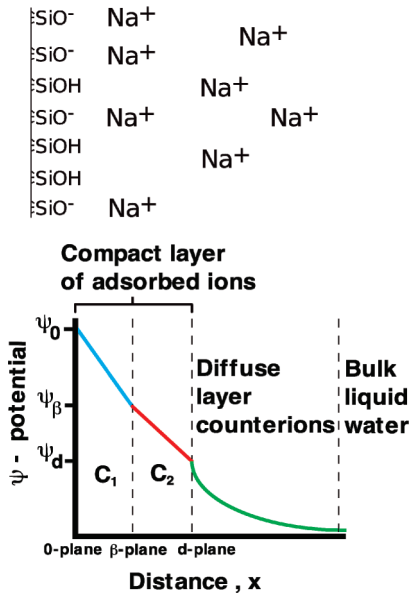

Figure 1. Schematic representation of the triple-layer model (TLM), one of the many SCMs used to describe the mineral/aqueous interface. The smallest potential determining ion in our system, H^+, adsorbs at the 0 plane, while the larger Na^+ adsorbs in a compact layer at the β plane and in a diffuse layer beginning at the d plane. The change in potential crossing the "proton capacitor" is ($V_H = \psi_0 - \psi_\beta$), the change in potential crossing the sodium capacitor is ($V_{Na} = \psi_\beta - \psi_d$), and the change in potential across the diffuse layer ψ_d. Note that distances from the surface are not to scale. Under our experimental conditions the diffuse layer is 3−30 nm long while the compact layers are less than 1 nm.

will be valid only at relatively low counterion concentrations (at elevated concentrations ion pairing is expected). The third requires that no partial dissolution or recrystallization of the surface occurs with changing aqueous phase chemistry. One such surface complexation model, the triple-layer model (TLM), is shown in Figure 1.

In an electrostatic sense, SCMs typically describe the neutralization of surface charge by a parallel plate capacitor(s) overlain by a layer of diffusely held counterions.[11−15] Chemically, the parallel plate capacitor(s) is formed by surface charge and specifically adsorbed counterions where each counterion adsorbs in a different layer as a function of its size and hydration (the first two layers to the left in Figure 1, upper panel). In this context specifically does not suggest a particular adsorption mechanism but rather only that the mechanism, whatever it is, is *specific* to a particular ion (i.e., all monovalent ions do not interact with a surface in the same way). Diffusely held counterions are adsorbed nonspecifically to neutralize the remaining charge (the third layer in Figure 1) and their density along the surface normal, an exponentially decaying concentration gradient with a length scale termed the Debye length (λ), is typically described by solution of the Poisson−Boltzmann equation.

Using an SCM to rationalize or predict trends in titration data, whether it be from simplified laboratory systems or more complicated natural samples, requires several parameters: at minimum the surface site density, a capacitance for each compact layer and equilibrium constants describing the adsorption of each potential determining ion. Initially, SCMs were applied in the environmental community with the goal of explaining the development of mineral surface charge as a function of pH of the adjoining aqueous phase. As might be expected from the large number of parameters, early work clarified that macroscopic titration data do not specify a unique molecular mechanism of adsorption.[16] Recently, however, a number of studies have either directly measured or calculated SCM parameters (with calculated results coming from molecular simulation or scaling relationships with bulk thermodynamic properties) and found that such independently determined parameters allow for accurate prediction of much titration and electrokinetic data.[17,18] Such results lend confidence to the notion that particular molecular mechanisms, postulated in the context of a particular SCM, are, in fact, physically meaningful. One interesting result of this exercise is that such calibrated SCMs appear able to reproduce titration results at values of pH and ionic strength that lie outside the calibration.[18]

One possible explanation for this range of applicability of SCMs is that while the atomic mechanism they contain is not accurate for individual surface/solute interactions, it remains true in an averaged sense. For example, a counterion may adsorb at only one type of surface site within a given pH range. Outside this range it may adsorb at multiple sites whose average adsorption energy equals that of the single adsorption site within the initial range. In what follows we describe limitations of SCM application to rationalize titration and surface potential data due to spatial averaging in silica mineral phases of well-defined nanoporosity.

Nanoporous silica is ubiquitous in the environment, of utility in a variety of (bio)technological applications, and straightforwardly synthesized using a 40 year old protocol of Stöber and others.[19−23] While natural porous colloidal silicas are expected to have a range both of pore and particle sizes, such variety considerably complicates the interpretation of experimental data and makes applications more difficult. Fortunately, Stöber type particles are known to be nearly monomodal with respect to particle and pore size. Much prior work has also demonstrated that this material is truly nanoporous: Stöber silica appears to have an effective pore diameter of <6 Å under vacuum and in solution.[20,21,23,24] These qualities make Stöber silica an attractive candidate for both the investigation of differential charge development on external and internal surfaces with changes in aqueous phase pH and for a variety of engineering applications.

Silica in general, and Stöber silica in particular, is a potentially unattractive candidate to gain general insight into ion adsorption to oxide surfaces because its surface has been argued to be relatively soft: multiple authors have suggested from light scattering, NMR, and rheological data that the surface of some types of silica at the silica/water interface is mechanically deformable, perhaps characterized by an array of silicic acid chains extending into solution, and that this "softness" is pH-dependent.[25−27] Such surface softness has not been observed for other oxide/water interfaces and has been argued to be the result of bulk silica's relatively low dielectric constant.[28] The possible existence of a soft surface for Stöber silica particles is problematic because electrokinetic methods of characterizing surface potential generally impose a pressure gradient parallel to the interface in excess of most experienced in the environment. The possibility then exists that the surface of these particles may be deformed by the measurement and that the resulting measured surface potential will differ from that of interest in most applications in a manner that is difficult to quantify. In this study we avoid this possible problem by measuring surface potential using a method that does not impose a shear stress on the interface.

More completely, we here report a series of acid/base titrations, NaCl titrations, and surface potential measurements of Stöber silica particle suspensions. Our work extends previous

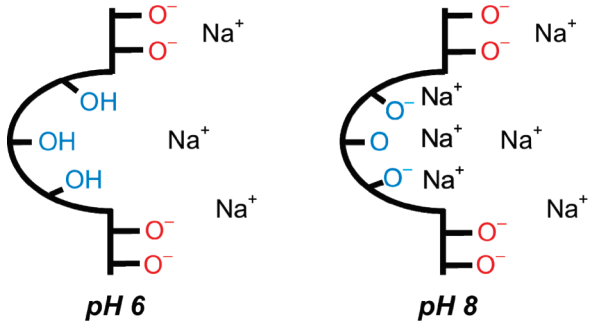

Figure 2. Silica surface at two pH environments. At pH 6, external surface sites (in red) are deprotonated and neutralized predominantly by a diffuse layer of counterions (Na^+); internal surface sites (in blue) are fully protonated. As pH increases, the internal surface sites are deprotonated and are neutralized by a specifically adsorbed layer of Na^+. No new net charge is developed on the external surface of the particle.

studies along these lines by both examining a larger range in pH and measuring surface potential using the nonlinear optical process of second harmonic generation (SHG). SHG allows for the *in situ* description of surface potential in stable colloidal suspensions with no additional shear forces imposed.[29,30] Consistent with Stöber silica's known nanoporosity, we measure surface proton loss with increasing pH in excess of that possible for nonporous materials using acid/base titrations of aqueous suspensions. Further, we find in salt titrations surface proton loss to be linearly related to counterion concentration (i.e., protons are effectively replaced by Na^+) above pH 6.5. Intriguingly, surface charge density, as inferred from the SHG surface potential measurement, is 10−15 times less than that suggested by titrations if every proton lost from the surface were to result in surface charge and above pH ≈ 6.5, is relatively independent of pH.

Taken together, these results support the following picture of deprotonation with increasing pH in suspensions of nanoporous oxides. As suspension pH is increased from the point of zero charge (pH_{pzc}: pH at which there is no net oxide surface charge) protons are lost to the aqueous phase, and this proton loss is apparent in acid/base titrations, occurs on external surfaces, and leads to surface charge development (as can be seen in nonzero surface potential). If more base is added to the suspension, protons continue to be lost to the aqueous phase (as is clear from acid/base titrations), but both salt titration measurements and surface potential measurements suggest that this proton loss does not lead to significant surface charge development. This qualitative change in the influence of proton desorption on surface charge with increasing pH (presumably applicable in general to the adsorption of small ions on nanoporous material, see Figure 2) suggests that for this type of material above this threshold pH the application of a traditional SCM to provide a framework for rationalizing or predicting ion adsorption and electrokinetic data is flawed. We further find that our measured external surface charge density, as inferred from the SHG surface potential measurements, agrees with the surface charge density calculated from conductivity measurements through plugs packed with porous silica particles.[22] The agreement of measured surface potential between methods that do and do not impose shear stress suggests that, in agreement with inferences from modeling aggregation data,[24] the surface of Stöber silica particles is not characterized by chains of poly(silicic acid).

These results should be useful to those interested in developing technological applications for nanoporous silica and are a cautionary lesson in the application of SCMs to natural, porous materials. Further, the results should increase confidence in the utility of SHG as a nondestructive probe of surface potential, a development of particular use in characterizing the electrical properties of soft, often biological, materials.

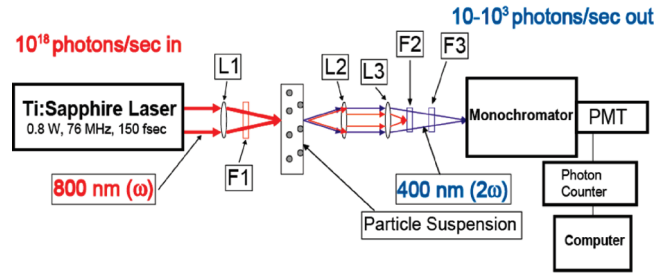

Figure 3. Schematic of experimental setup and parameters for SHG experiments including laser parameters and approximate efficiency of process. L1, L2, and L3 are lenses, F1 is a red transmitting, blue blocking filter, and F2 and F3 are blue transmitting, red blocking filters.

II. Methods

Silica particles, with a diameter of 1 μm, synthesized by a low-temperature Stöber protocol, were purchased from Alfa-Aesar and used as received. Solutions were created using reagent grade NaOH (Fisher, ACS Certified), NaCl (J.T. Baker, ACS Reagent), HCl (Fisher, ACS Certified), and redistilled Millipore (>18.2 MΩ·cm) ultrapure water. Samples for optical analysis and titration had concentrations of 10^9 and 10^{11} particles/mL, respectively. Stability of the suspensions used in the SHG analyses was verified by the stability of the SHG signal over time scales in excess of the measurement period, by measurement of optical attenuation (in a JASCO V-530 UV/vis spectrophotometer) at both 400 and 800 nm as a function of changing pH and salt concentration, and through measurement of particle size (via dynamic light scattering using a Brookhaven 90 plus particle size analyzer) of suspensions of particles over several days.

Surface area analyses of multiple samples by N_2 adsorption (using the method of Brunauer, Emmett, and Teller,[31] in a Micrometrics ASAP 2020) gave a sample surface area of 5.15 ± 0.2 m^2/g, in approximate agreement both with the geometric surface area calculated assuming the manufacturer's particle radius and with the geometric surface area as estimated from AFM measurements (Molecular Imaging, Pico Plus) of a particle suspension deposited on mica and dried in air.

The SHG measurements employed a tunable Ti:sapphire oscillator (Coherent Mira 900) pumped by an Ar ion laser (Coherent Innova 310). The pulsed output of the Ti/sapphire laser had a repetition rate of 76 MHz, a duration of 150 fs, a center wavelength of 800 nm, and a bandwidth of 7 nm (full width at half-maximum). The light from the Ti:sapphire laser was focused, filtered to remove 400 nm photons, sent through a 2 mm path length quartz cuvette containing a suspension of silica particles, collimated, filtered to remove 800 nm light, and focused into a monochromator, which directed 400 nm photons to a photomultiplier tube (PMT) and a gated photon counter. The system is shown in Figure 3 along with the process' estimated efficiency. The average power of the 800 nm laser beam at the sample was 480 mW (i.e., 6.3 nJ/pulse).

Titrations were carried out following the procedure described by Zelazny et al.[32] where the titrant was either concentrated NaCl or NaOH. For all titrations samples were allowed to equilibrate for 24 h before analysis and purged using N_2 for 10

min prior to and during the experiment. After each addition of NaOH or NaCl the sample was allowed to equilibrate for 2 min before measurement of pH.

Above pH 8 the dissolution of silica becomes thermodynamically favorable.[9] However, measurement of dissolved silica for all the experimental conditions reported here showed no detectable dissolution over the time scales of our experiments. In these control experiments dissolved silica was quantified using the colorimetric procedure of Strickland et al.[33]

Before model fitting, raw SHG intensities were corrected for hyper-Rayleigh scattering from pure water and attenuation of 800 and 400 nm light by particles using a calibration curve created by measuring attenuation in a series of samples of increasing particle concentration in a JASCO V-530 UV/vis spectrophotometer. Model fitting was carried out using an approach in which 8000 initial guesses, spanning at least 2 orders of magnitude in each model parameter, were tried and the results with the lowest reduced χ^2 reported. Estimated error in model parameters was calculated by averaging parameters resulting from best fits to multiple independent experiments. All optimization of model parameters with respect to data was performed using the Levenberg−Marquardt algorithm as implemented in the Igor Pro software package (Wavemetrics, Inc.).

III. Results and Discussion

Much prior work has argued that, with increasing pH, deprotonation of the silica surface (without regard to its porosity) occurs at one surface site and can be written

$$\rangle \mathrm{SiOH} \leftrightarrow \rangle \mathrm{SiO}^- + \mathrm{H}^+ \quad (1)$$

It is clear that the loss of protons from the silica surface with increasing pH also depends on the type of counterion present in solution.[34,35] For our experimental system, experiments performed in NaCl, this dependence can be represented (in which the notation $\rangle$Si−O···Na represents a specifically adsorbed Na^+ but should not be taken to suggest inner-sphere adsorption)

$$\rangle \mathrm{SiO}\cdots\mathrm{Na} \leftrightarrow \rangle \mathrm{SiO}^- + \mathrm{Na}^+ \quad (2)$$

Representative results for acid/base titrations are shown in Figure 4. Qualitatively, these results are similar to previous experiments describing titrations of the nonporous silica/water system: surface proton loss is relatively low from pH = 2 to pH = 6 and increases rapidly thereafter.[27,34−38] Much prior experimental work on various types of nonporous silica has suggested that the maximum number of deprotonateable surface sites is 4.6−4.9 sites/nm^2, where the surface site density is determined by gas adsorption (typically N_2) in conjunction with tritium exchange or crystallographic considerations.[18,39] As is clear from inspection of Figure 4, the measured surface proton loss per unit BET-N_2 surface area from Stöber silica particles exceeds this presumed physical limit (e.g., for pH > 7 and 0.1 M NaCl more than 10 sites/nm^2).

This possible inconsistency can be overcome by considering the nanoporous structure of Stöber silica. Prior studies employing gas adsorption under vacuum with gases of varying size (He, Ar, N_2, Xe, and Kr), dielectric impedance measurements on slurries with bases, and counterions of varying size and limited titrations using bases of varying size suggest that this material has a single well-defined porosity with pores of size 3−5 Å.[21,23,40] In agreement with this prior work, we find that

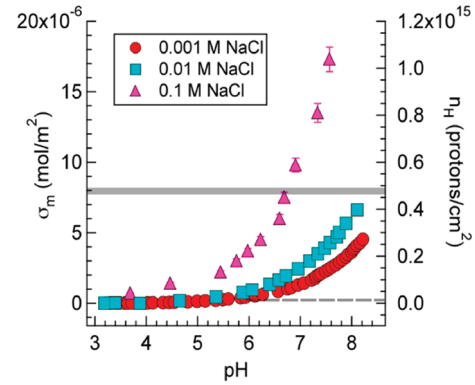

Figure 4. Titrations of Stöber silica particles using 0.1, 0.01, and 0.001 mol/L NaCl from acidic to basic conditions as a function of pH and relative to moles of protons lost from the surface per m^2 is (σ_M) and the number of protons lost from the surface per cm^2 (n_H). Uncertainty indicated is the estimated analytical error in single measurements. As noted in prior studies (and discussed in the text) the reproducibility of titrations of this material with 0.1 and 0.01 mol/L NaCl was substantially reduced. The solid horizontal line is 4.6−4.9 sites/nm^2 (or a maximum number of protons lost from the surface of (0.46−0.49) × 10^{15} cm^{-2}), the maximum surface site density of amorphous silica. The dashed line is the amount of protons lost from the surface that would be required to generate the surface charge density observed by SHG above pH 6.

pores of such size allow H^+/OH^- and Na^+ access to internal surface area in solution but restrict access of N_2 under vacuum. Thus, the apparent inconsistency identified in the previous paragraph is the result of N_2 having a different accessible surface area than the Na^+, H^+, or OH^- ions. Estimates of the internal surface area relative to the external (i.e., internal area: external area) are difficult and may be particle size dependent but range from 2 to 10.[23] Presumably as a result of this pore structure hindering diffusion of protons and counterions to/from the surface, and in agreement with prior studies, we found significant hysteresis in our initial attempts to both forward and backward titrate (i.e., titrate acidic → basic → acidic) particle suspensions.[24]

Salt titrations were also performed at initial pHs of 10.9 and 7.2 (in which an aqueous solution of concentrated NaCl was the titrant and changes in pH were recorded after addition of each titrant aliquot). In each case, the addition of salt leads to a decrease in bulk pH. After subtracting the reference and normalizing with respect to the BET-N_2 surface area, representative titrations at each pH are shown in Figure 5. Of note here is that surface proton loss increases (i.e., bulk solution [H^+] decreases) linearly with increasing salt concentration. For an idealized, nonporous, silica surface this result is unexpected. Increasing the concentration of Na^+ ions should allow the more effective screening of charged groups at the surface up to some saturation point: surface proton loss should asymptotically approach some limit with increasing salt concentration. Rationalizing the absence of this limit requires us to consider the effect of porosity on the structure of the electrical double layer in the neighboring aqueous phase.

A quantitative description of the electrical double layer requires relating counterion concentration and surface potential/charge. As discussed above, for nonporous surfaces at low potential and/or low counterion concentration, surface charge neutralization is thought to occur via a layer of diffusely held counterions whose distribution, normal to the surface, is modeled by solution of the Poisson−Boltzmann equation—the Gouy−Chapman model—and the resulting length scale over which charge is neutralized—is termed the Debye length. At higher

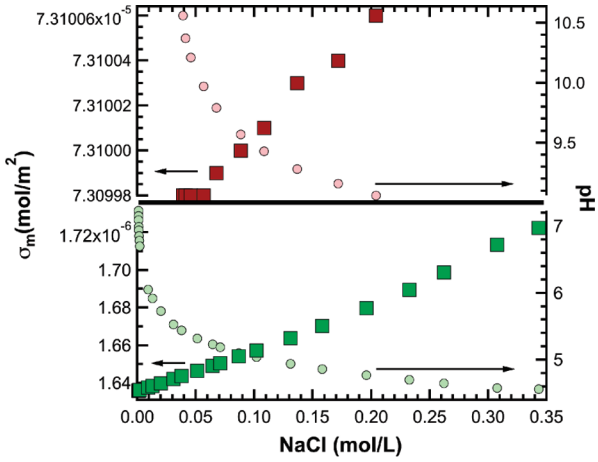

Figure 5. Salt titrations at two different initial pH values. For each titration the left-hand axis (and the squares) shows the loss of protons per unit silica surface area while the right-hand axis (and the circles) shows change in pH of the bulk aqueous phase with added salt. Both titrations show linear loss of protons from the surface with increasing salt concentration. As shown on the right-hand axes, the titration in the upper panel (pink circles) was begun at a higher pH than that in the lower panel (light green circles). Particle surface area for normalization of surface proton loss was determined by BET-N_2 adsorption.

surface charge and/or higher counterion concentration, a portion of the system's counterions adsorb specifically to the surface and are described in electrostatic terms as forming a molecularly thick layer of constant capacitance (Figure 1). Most modern approaches to surface complexation modeling further postulate separate layers for different types of counterions (motivated by the notion that some counterions, because of their different radii or degree of hydration, can more closely approach the surface than others: that the mechanism of the specific adsorption of counterions depends on the counterion).[18,41,42] In general, the thickness of the diffuse layer is 100 times greater than the compact layer(s) (in 0.1−10 mM NaCl the Debye Length is 30−3 nm vs ~6 Å for each compact layer[54]).

For particles with a large internal/external surface area ratio, such as Stöber silica, the number of counterions within the particle is expected to be far greater than the number at the particle's external surface. As discussed above, the usual SCM approach assumes that specifically adsorbed counterions are overlain by a cloud of diffusely held counterions. However, for particles with significant internal surface area, and significant counterion concentration and/or surface site density, counterions in the external diffuse layer are quantitatively unimportant in describing ion adsorption. If pore diameters are small relative to the Debye length, there are no gradients in potential parallel to the pore surface and counterion distribution within the particle (given a particle porosity as a function of distance from the liquid phase) can be described using a simple adsorption model (i.e., there is no local electrostatic contribution to the free energy of adsorption). Determining the relationship of counterion adsorption and particle surface potential (i.e., understanding the potential gradient normal to the external particle surface) for this case requires simultaneously solving an adsorption model and the Poisson equation.

In a prior study Lyklema took this approach, solving the so-called Poisson−Langmuir equation in which the counterion density is defined by the pore distribution in the solid phase and the Langmuir isotherm for an idealized porous material.[43] In this model, for relatively high counterion concentration and/or surface potential, changing pH or increasing counterion concentration generates insignificant new surface charge (internal or external). Put another way, for every deprotonated $\rangle SiO^-$ group, an $\rangle SiO\cdots Na$ group is created; i.e., protons are replaced by sodium ions, resulting in a linear relationship between surface proton loss and Na^+ concentration, in agreement with our observations (Figure 5). Because the internal surface area of such systems generally far exceeds the external, titrations of mineral phases using ions small enough to penetrate the pores tell us about the internal surface chemistry: the proton loss signal from internal surfaces overwhelms that from external. If titration data are dominated by ions interacting with internal surfaces, surface complexation models appropriate for nonporous mineral surfaces (e.g., the triple-layer model) are no longer applicable. Furthermore, these data tell us little about how different particles interact with each other or how ions too large to fit into pores adsorb on external surfaces. (In both situations the chemistry and charge of the external surface, which need not be electrically neutral, are important.)

We measured the external surface potential (and calculated the external surface charge) using second harmonic generation (SHG), a second-order optical process in which a sample is irradiated by photons (of frequency ω_1) resulting in the emission of photons of frequency $2\omega_1 = \omega_2$. SHG is inherently surface sensitive and has been demonstrated in prior studies of colloidal suspensions, emulsions, the planar silica/water interface, and functionalized glass slides to be enhanced at high surface potential due to a third-order contribution to the SHG process.[29,30,44−50] Both our salt titration data and prior electrokinetic measurements suggest charge development occurs on the external surface of Stöber silica particles.[21,22]

Following prior workers,[44] we here model the change in I_{SHG} with change in aqueous phase NaCl concentration as

$$I_{SHG} \propto |A + B\psi_0|^2 \quad (3)$$

where A and B are a function of interfacial water density, orientation, nonresonant water hyperpolarizability (second and third order), and the appropriate Fresnel factors for a particular experimental setup. Finally, ϕ_0 is the surface potential (where the relevant surface here is that defined by a layer of undercoordinated oxygens). Extensive X-ray reflection, fluorescence, and absorption studies suggest that for the oxide/water system interfacial water densities and orientation do not change significantly with moderate changes in bulk ionic strength.[51] Finally, as nonresonant molecular hyperpolarizabilites in general (and water in particular) are known to be relatively insensitive to both small changes in ionic strength in aqueous solution and applied dc fields of the amplitude imposed by the interface in our system, we here treat A and B as empirical constants and determine them from fits to the data. As discussed above, for the silica/water interface there is extensive evidence that the surface potential can change due the adsorption of a wide variety of ions. Because the effect of ion adsorption on surface potential is a function of the adsorption mechanism (specific/nonspecific, if specific how close to the surface) to describe the influence of ion adsorption on surface potential requires a model able to accommodate these differences. The triple-layer model (shown in Figure 1) is one such model. Thus, by referring to Figure 1, we can rewrite ψ_0 in terms of its components (in which $V_H = \psi_0 - \psi_\beta$: the change in potential across the proton capacitor; $V_{Na} = \psi_\beta - \psi_d$: the change in potential across the sodium capacitor and, because the potential of bulk water is zero, the change in potential across the diffuse layer is ψ_d)

$$I_{SHG} \propto |A + B\{V_H + V_{Na} + \psi_d\}|^2 \quad (4)$$

Further reference to Figure 1 hopefully makes clear that V_H is a function of the concentration of silanol groups ($V_H = V_H([\rangle SiOH])$, V_{Na} is a function of the concentration of specifically adsorbed sodium ions ($V_{Na} = V_{Na}([\rangle SiO\cdots Na])$), and ψ_d is a function of both the concentration of deprotonated silanol groups and the bulk concentration of NaCl ($\psi_d = \psi_d([\rangle SiO^-], [NaCl])$). Inspection of the acid/base titration curve at 0.001 M NaCl in Figure 4 makes clear that if we titrate a solution containing silica particles from pH 4.6 to 7.4 (in the presence of 0.001 M NaCl) by adding base, we lose $\approx 1.6 \times 10^{-6}$ mol/m^2 of protons from the silica surface. In contrast, the lower panel of Figure 5 demonstrates that if start with a suspension of silica particles at pH 7.4 (and 0 M NaCl) and proceed to increase the concentration of NaCl from 0 to 0.35 M, we can cause pH to change back to 4.6 while losing only an additional 0.08×10^{-6} mol/m^2 from the silica surface. The loss of protons from the silica surface results in a decrease in [⟩SiOH] (i.e., a decreasing V_H) and an increase in either [⟩SiO···Na] (i.e., V_{Na}) or [⟩SiO$^-$] (i.e., ψ_d), or both. The comparison of Figures 4 and 5 highlighted above suggests that adding OH$^-$ to the bulk solution is an extremely efficient way to change surface chemical speciation while adding NaCl is not. If the change in surface chemical speciation is small while adding NaCl, this suggests that it is reasonable to follow Ong, Zhao, and Eisenthal's approach (see ref 44) and to model the effect of adding NaCl on surface potential as a change in surface screening due to the presence of a loosely held cloud of Na$^+$ counterions. This is equivalent to when modeling the change in I_{SHG} due to change in [NaCl], simplifying eq 4 to read

$$I_{SHG} \propto |A + B\psi_d|^2 \quad (5)$$

Given constant A and B and changing Na$^+$ concentration, the diffuse plane surface potential (ψ_d) can be related to the diffuse plane charge density using the Gouy−Chapman equation

$$I_{SHG} = \left|A + B\frac{2\pi}{\beta e}\sinh^{-1}\left([\rangle SiO^-]\sqrt{\frac{\beta}{2\varepsilon\varepsilon_0[NaCl]}}\right)\right|^2 \quad (6)$$

in which $\beta = 1/(kT)$, ε is the bulk dielectric constant of water, ε_0 is the permittivity of free space, [NaCl] is the bulk concentration of Na$^+$, and [⟩SiO$^-$] is silica surface charge neutralized by counterions held in the diffuse layer.[29]

In using eq 6 to model the change in measured SHG intensity with changing Na$^+$ concentration, we are assuming that charge density at the diffuse plane (i.e., [⟩SiO$^-$]) does not change as a function of Na$^+$ concentration: that the diffuse plane under these conditions is a constant charge interface. This assumption is consistent with our salt titration results, which imply that surface deprotonation is compensated by Na$^+$ adsorption at pHs in excess of 6 (i.e., increasing the concentration of NaCl in bulk results in an exchange of ⟩SiOH surface groups for ⟩SiO···Na without significantly increasing the number of ⟩SiO$^-$), and is supported by prior AFM studies of the interaction of silica colloids and plates.[52]

A representative SHG salt titration is shown in Figure 6. We performed similar titrations with initial pH values of ∼7.2, 8, and 10.1 (adding salt up to 1 M causes the pH in the SHG experiments to decrease by ∼0.75 pH units). Qualitatively, all

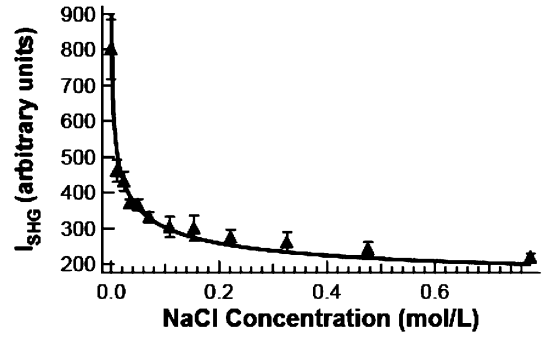

Figure 6. A representative plot of variation of I_{SHG} with change in NaCl concentration. The experiment shown had an initial pH of ∼7.9 and a particle concentration of 10^9 particles/mL. Error indicates counting reproducibility for this sample. Solid line is fit to the model in eq 4.

curves look the same and are similar to those measured for other systems:[29,30,44,45,53] exponentially decreasing as a function of added salt. Fitting each set of titration curves using eq 6 gives a diffuse layer charge density of 0.022 ± 0.014, 0.028 ± 0.022, and 0.035 ± 0.022 C/m^2 (for multiple salt titrations from initial pHs of 7.2, 8, and 10). To within experimental uncertainty, this value agrees with the charge density of 0.055 C/m^2 at pH 9, measured by Minor et al.[24] using conductivity measurements through plugs packed with 300 nm Stöber silica particles.

Both our value and the Minor et al. value of the surface charge are less than 5% of the charge that might be expected to accumulate on the surface of a nonporous silica if all protons lost resulted in surface charge (i.e., if the reaction ⟩Si−OH ↔ Si−O$^-$ + H$^+$ is much more favorable than ⟩Si−O$^-$ + Na$^+$ ↔ Si−O···Na). For silica that has a surface hydroxyl density of 4 sites/nm^2 the conversion of all sites to >SiO$^-$ would result in a charge density of 0.64 C/m^2, well in excess of our measured 0.022−0.035. Furthermore, as illustrated in Figure 4, proton loss from the surface appears to be increasing exponentially through the pH range of the SHG titrations. Thus, relative to the acid/base titration results, our SHG data within experimental uncertainty are consistent with a scenario in which [⟩SiO$^-$], at pHs greater than 6.5, is insensitive to pH.

The observation that [⟩SiO$^-$] appears to be relatively insensitive to pH above ∼6.5 in our SHG measurements (Figure 6) but that proton loss continues with increasing pH (Figure 4), for which Na$^+$ compensates (as concluded from the salt titration, see Figure 5, and discussion above), is consistent with Stöber silica particles in this pH range having small electrically saturated pores. As our SHG (Figure 6) and prior conductivity measurements suggest that the external surface retains a relatively constant charge with increasing pH, the chemistry of the internal and external surfaces are decoupled: deprotonation and Na$^+$ adsorption on internal surfaces can be rationalized without accounting for charge on the external surface neutralized by diffusely held counterions. This decoupling implies that conventional SCMs no longer provide a coherent framework for rationalizing titration and electrokinetic measurements. Furthermore, as the external surface is the relevant parameter for describing the stability of colloidal suspensions and the adsorption of ions sterically excluded from the particle interior, our observed decoupling highlights the necessity of understanding this critical pH threshold for nanoporous materials.

The notion that there is a pH for the silica/water interface, above which [⟩SiO$^-$] or diffuse layer charge does not increase, qualitatively agrees with previous streaming potential, electrophoretic mobility, and AFM studies of both the nonporous and nanoporous silica/water interface.[54−57] For example, Scales et

al. found, in a streaming potential study of the (nonporous) silica/water interface as a function of pH and ionic strength, two distinct regimes: below pH 7 surface potential was a function of both pH and ionic strength, while above this threshold pH surface potential depended only on ionic strength.[54] Similarly, Zhang et al. found that surface charge inferred from an AFM measurement for both non- and nanoporous silica appeared to saturate as a function of pH above ≈7.[57] These types of measurements are generally interpreted as providing insight into diffuse layer charge/potential (i.e., [⟩SiO$^-$]/ψ_d).

On the other hand, if all protons lost from the surface result in surface charge, prior titration studies of the nonporous silica/water interface appear to disagree with the notion that there is some critical pH above which surface charge at the silica/water interface does not increase. In general, these sorts of measurements show no saturation or plateau in surface proton loss with increasing pH.[18,27,35]

Finally, prior optical studies of the planar non- and nanoporous silica/water interface as a function of pH (at relatively high ionic strength) using both nonresonant second harmonic generation spectroscopy and sum frequency generation spectroscopy resonant with the OH stretch of interfacial H_2O show no plateau in second harmonic or sum frequency spectral amplitude at pH 6 (spectral intensity appears to increase up to pH 11).[44,57−59] These studies have been interpreted to suggest that surface charging continues well above pH 7.

To summarize, both our optical measurements at low ionic strength and various types of electrokinetic measurements and AFM studies of the silica/water interface all appear to support the notion that there is some crtitical pH above which the surface charge of the silica/water interface (i.e., [⟩SiO$^-$]) does not increase. Simultaneously, it is clear that there is no such threshold for surface proton loss (in an acid/base titration) or spectral amplitude in either second harmonic (at high ionic strength) or sum frequency measurements (when spectra are collected with increasing bulk pH). These apparently contradictory observations can be reconciled using logic initially laid out (for the interpretation of the second harmonic signal from charged interfaces) by Ong et al.[44] As they noted, and as was discussed above, at relatively high ionic strength the diffuse portion of the electrical double layer is known to collapse and double-layer structure is composed of a layer of specifically adsorbed counterions (in our and their case Na^+) which, in conjunction with the surface charge, form a parallel plate capacitor. For such systems most of the potential drop (as one moves away from the interface and into the liquid) happens within the capacitor, and thus SHG and SFG spectral amplitudes are a function of ψ_0 or ψ_β (and no longer ψ_d). Taken together, both our and prior studies are consistent with a scenario in which, with increasing pH at the silica/water interface, [⟩SiO$^-$] saturates. Above this critical pH surface proton loss continues but is compensated by specific counterion adsorption: in our case ⟩SiOH groups are substituted by ⟩SiO$\cdots$Na$^+$. Because Na^+ is large relative to the proton and because it may remain hydrated at the interface, the interfacial capacitor in which Na is the counterion supports an increased surface potential from that in which the proton is the counterion. This implies that surface potential, and hence SHG and SFG spectral amplitudes, may continue to increase, even as [⟩SiO$^-$] remains constant.

This mechanism is shown in cartoon form in Figure 7. At low pH and low ionic strength (panel A) the Debye length is large, the surface is relatively protonated ($(\psi_0 - \psi_\beta) > (\psi_\beta - \psi_d)$), and the diffuse layer potential (ψ_d) is relatively large. Because the third-order contribution to I_{SHG} scales with the

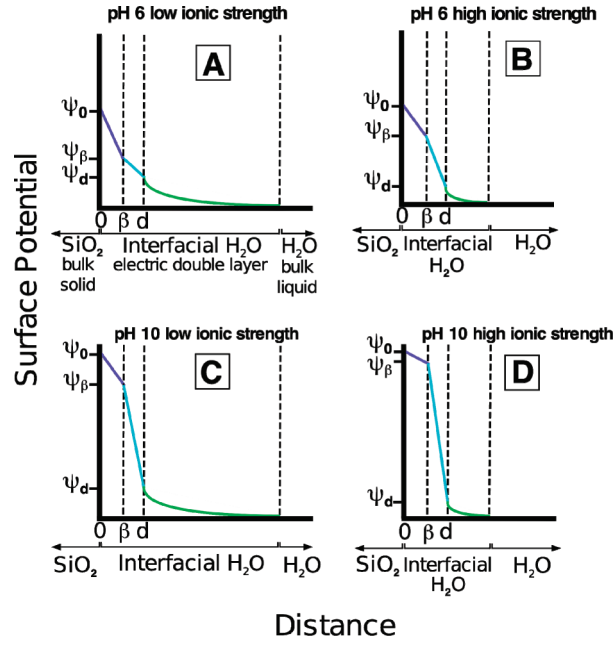

Figure 7. Cartoon description of changing relative surface potentials as a function of pH and ionic strength. With the collapse of the diffuse layer shown in transition from low to high ionic strength (at either pH) I_{SHG} becomes a function of ψ_0 and/or ψ_β at low pH (where $(\psi_0 - \psi_\beta)$ and $(\psi_\beta - \psi_d)$ are approximately equal and large relative to ψ_d) and a function of ψ_β at high pH, where the surface chemistry is dominated by specifically adsorbed Na^+.

number of water molecules in the electrical double layer, and because for this situation the great majority of water molecules in the electrical double layer are in the diffuse layer, I_{SHG} is relatively large and is a function of the diffuse layer potential (as shown in eq 3). At low pH and high ionic strength (panel B), the Debye length is relatively small; the surface is relatively deprotonated ($(\psi_0 - \psi_\beta) \approx (\psi_\beta - \psi_d)$) and the diffuse layer potential decreased. Because under these conditions the diffuse layer has collapsed, I_{SHG} is a function of ψ_0 and/or ψ_β and, because of the relatively small number of water affected by the surface potential, less than in the low salt case. At high pH and low ionic strength (panel C) the Debye length is relatively large, the total potential moving from the surface to the bulk is larger than for the low pH cases (ψ_0(high pH) > ψ_0(low pH)), and the surface is deprotonated relative to low pH conditions ($(\psi_0 - \psi_\beta) < (\psi_\beta - \psi_d)$). For much the same reason as for the low pH, low ionic strength case I_{SHG} is here a function of ψ_d (as shown in eq 3). For the final high pH, high ionic strength case (panel D) the Debye length is now small, the total potential moving from the surface to the bulk is larger than for the low pH cases (ψ_0(high pH) > ψ_0(low pH)), and the surface deprotonated to an even larger degree ($(\psi_0 - \psi_\beta) \ll (\psi_\beta - \psi_d)$). Under these conditions I_{SHG} is a function of ψ_β and, because of the dramatically smaller number of water molecules effected by the surface field, less than in the low salt case.

As described above, our SHG measurements of [>SiO$^-$] agree with those obtained from conductivity measurements through packed plugs of Stöber silica. These two means of measuring surface charge differ in the shear stress imposed on the interface during the measurement and in the extent to which individual particles interact with each other: both effects are present in the conductivity measurement through a porous plug but absent in the SHG. As these two methods agree, and both sheer stress and particle/particle interaction would be expected to perturb any rheologically soft interfacial layer of silica present in the

conductivity measurement, it seems unlikely that the water/Stöber silica interface has such deformable interfacial structure. This conclusion agrees with that of prior workers from particle aggregation data.[24]

IV. Summary and Conclusions

In this study we performed acid/base titrations, NaCl titrations, and surface potential measurements using SHG, of Stöber silica suspensions. In agreement with prior studies, our results are most easily understood as suggesting that this material has extensive nanoporosity: pores that are sufficiently large to allow the penetration of potential determining ions (H^+/OH^- and Na^+) into the interior of the particle while in solution and sufficiently small to preclude the penetration of N_2 in a vacuum. In agreement with predictions from prior theoretical work, we find that at sufficiently high pH the relationship of protons lost from the surface to Na^+ in solution is linear. This observation is consistent with proton loss from the surface being perfectly compensated by the adsorption of Na^+ above a critical pH $\approx$6.5.

Such compensation implies that, above this threshold pH, the charge of a particle surface is not related to proton loss and, therefore, that SCMs will fail. Direct measurements of surface potential over a range of pH values, using SHG, a noninvasive optical approach, confirm this conclusion as particle surface charge is relatively constant at pH values above $\approx$6.5 even as proton loss from the mineral particle surface continues. Some types of silica appear to possess a surface layer at the silica/water interface that is rheologically soft. The fact that our measurement of external surface charge using SHG agrees with that inferred from measurements of conductivity through porous plugs composed of the same types of silica by prior authors suggests that Stöber particles are unlikely to have such a soft surface.[22] The same conclusion has also been reached less directly through modeling of aggregation rate measurements of suspensions of Stöber silica particles.[24]

Traditionally, surface charge/potential is measured using electrokinetic techniques that impose shear stress on the mineral surface. SHG avoids this possible artifact and, as illustrated by its prior application to measurement of the surface potential of liposomes,[30] allows accurate determination of the charge of soft, deformable, surfaces. Our results should engender confidence that this approach may be usefully applied to measurement of surface charging for amorphous, rough mineral phases whose surface morphology may be significantly altered under stress.

Finally, our results highlight the importance of using apparent surface charge measured from acid/base titrations with caution in describing the interaction of porous particles and adsorption on porous mineral phases. As described above for our nanoporous silica, at pHs sufficiently far from the pH point of zero charge, the chemistry of proton loss becomes effectively decoupled from that of surface charge.

Acknowledgment. We thank Professor Adrienne Cooper for use of the Micrometrics ASAP 2020 instrument, Dr. Kyoungja Seo for her assistance with the AFM measurements, and Ali Eftekhari-Bafrooei, Oleksandr Isaienko, and Professor Jim Kubicki for valuable discussions. This work was supported by the Department of Energy, Office of Basic Energy Science, and by the Center for Environmental Kinetics Analysis at Penn State (which is supported by the US National Science Foundation under Grant CHE-0431328).

References and Notes

(1) O'Day, P. A.; Carroll, S. A.; Randall, S.; Martinelli, R. E.; Anderson, S. L.; Jelinski, J.; Knezovich, J. P. *Environ. Sci. Technol.* **2000**, *34*, 3665–3673.

(2) Fontaine, S.; Barot, S.; Barré, P.; Bdioui, N.; Mary, B.; Rumpel, C. *Nature* **2007**, *450* (8), 277–281.

(3) Galy, V.; France-Lanord, C.; Beyssac, O.; Faure, P.; Kudrass, H.; Palhol, F. *Nature* **2007**, *450* (15), 407–411.

(4) Hazen, R. M.; Filley, T. R.; Goodfriend, G. A. *Proc. Natl. Acad. Sci. U.S.A.* **2001**, *98* (10), 5487–5490.

(5) Hazen, R. M.; Sholl, D. S. *Nature Mater.* **2003**, *2* (6), 367–374.

(6) Contreras, R.; Sahlin, H.; Frangos, J. A. *J. Biomed. Mater. Res., Part A* **2007**, *80A* (2), 480–485.

(7) McCarthy, J. F.; Degueldre, C. Sampling and Characterization of Colloids and Particles in Groundwater for Studying Their Role in Contaminant Transport. In *Environmental Particles*; Buffle, J., van Leeuwen, H. P., Eds.; Lewis Publishers: Boca Raton, FL, 1993; Vol. 2, pp 247−315.

(8) McCarthy, J. F.; McKay, L. D. *Vadose Zone J.* **2004**, *3* (2), 326–337.

(9) Stumm, W.; Morgan, J. J. *Aquatic Chemistry: Chemical Equilibria and Rates in Natural Water*; Wiley: New York, 1996; p 1022.

(10) Sposito, G. *Chimia* **1989**, *43* (6), 169–176.

(11) Schindler, P. W. *Kolloid Z. Z. Polym.* **1972**, *250*, 759.

(12) Huang, C.-P.; Stumm, W. *J. Colloid Interface Sci.* **1973**, *43* (2), 409–420.

(13) Yates, D. E.; Levine, S.; Healy, T. W. *J. Chem. Soc., Faraday Trans. 1* **1974**, *70*, 1807–1818.

(14) Davis, J. A.; James, R. O.; Leckie, J. O. *J. Colloid Interface Sci.* **1978**, *63* (3), 480–499.

(15) Davis, J. A.; Leckie, J. O. *J. Colloid Interface Sci.* **1978**, *67* (1), 90–107.

(16) Westall, J.; Hohl, H. *Adv. Colloid Interface Sci.* **1980**, *12*, 265–294.

(17) Zhang, Z.; Fenter, P.; Cheng, L.; Sturchio, N. C.; Bedzyk, M. J.; Predota, M.; Bandura, A.; Kubicki, J. D.; Lvov, S. N.; Cummings, P. T.; Chialvo, A. A.; Ridley, M. K.; Benezeth, P.; Anovitz, L.; Palmer, D. A.; Machesky, M. L.; Wesolowski, D. J. *Langmuir* **2004**, *20* (12), 4954–4969.

(18) Sverjensky, D. A. *Geochim. Cosmochim. Acta* **2005**, *69* (2), 225–257.

(19) Stöber, W.; Fink, A.; Bohn, E. *J. Colloid Interface Sci.* **1968**, *26* (1), 62–69.

(20) Gallas, J. P.; Lavalley, J. C.; Burneau, A.; Barres, O. *Langmuir* **1991**, *7* (6), 1235–1240.

(21) de Keizer, A.; van der Ent, E. M.; Koopal, L. K. *Colloids Surf., A* **1998**, *142* (2−3), 303–313.

(22) Minor, M.; van der Linde, A. J.; van Leeuwen, H. P.; Lyklema, J. *Colloids Surf., A* **1998**, *142* (2−3), 165–173.

(23) Despas, C.; Walcarius, A.; Bessiere, J. *Langmuir* **1999**, *15* (9), 3186–3196.

(24) Kobayashi, M.; Skarba, M.; Galletto, P.; Cakara, D.; Borkovec, M. *J. Colloid Interface Sci.* **2005**, *292* (1), 139–147.

(25) Vigil, G.; Xu, Z. H.; Steinberg, S.; Israelachvili, J. *J. Colloid Interface Sci.* **1994**, *165* (2), 367–385.

(26) Carroll, S. A.; Maxwell, R. S.; Bourcier, W.; Martin, S.; Hulsey, S. *Geochim. Cosmochim. Acta* **2002**, *66* (6), 913–926.

(27) Kobayashi, M.; Juillerat, F.; Galletto, P.; Bowen, P.; Borkovec, M. *Langmuir* **2005**, *21* (13), 5761–5769.

(28) Sahai, N. *Environ. Sci. Technol.* **2002**, *36* (3), 445–452.

(29) Yan, E. C. Y.; Liu, Y.; Eisenthal, K. B. *J. Phys. Chem. B* **1998**, *102* (33), 6331–6336.

(30) Liu, Y.; Yan, C. Y.; Zhao, X. L.; Eisenthal, K. B. *Langmuir* **2001**, *17* (7), 2063–2066.

(31) Brunauer, S.; Emmett, P. H.; Teller, E. *J. Am. Chem. Soc.* **1938**, *60*, 309–319.

(32) Zelazny, L. W.; He, L.; Vanwormhoudt, A. An Analysis of Soils and Anion Exchange. In *Methods of Soil Analysis Part 3: Chemical Methods*; Soil Science Society of America and American Society of Agronomy: 1996; Vol. 5, pp 1249−1250.

(33) Strickland, J. D. H.; Parsons, T. R. Determination of Reactive Silicate. In *A Practical Handbook of Seawater Analysis*; Fisheries Research Board of Canada: Ottawa, 1972; pp 65−70.

(34) Karlsson, M.; Craven, C.; Dove, P. M.; Casey, W. H. *Aquat. Geochem.* **2001**, *7* (1), 13–32.

(35) Dove, P. M.; Craven, C. M. *Geochim. Cosmochim. Acta* **2005**, *69* (21), 4963–4970.

(36) Tadros, T. F.; Lyklema, J. *J. Electroanal. Chem.* **1968**, *17* (3−4), 267.

(37) Tadros, T. F.; Lyklema, J. *J. Electroanal. Chem.* **1969**, *22* (1), 1–7.

(38) Yates, D. E.; Healy, T. W. *J. Colloid Interface Sci.* **1976**, *55* (1), 9–19.

(39) Zhuravlev, L. T. *Colloids Surf., A* **2000**, *173*, 1–38.

(40) Giesche, H. *J. Eur. Ceram. Soc.* **1994**, *14* (3), 189–204.

(41) Hiemstra, T.; Van Riemsdijk, W. H. *Colloids Surf.* **1991**, *59*, 7–25.

(42) Hiemstra, T.; Van Riemsdijk, W. H. *J. Colloid Interface Sci.* **1996**, *179* (2), 488–508.

(43) Lyklema, J. *J. Electroanal. Chem.* **1968**, *18* (4), 341–348.
(44) Ong, S.; Zhao, X.; Eisenthal, K. B. *Chem. Phys. Lett.* **1992**, *191* (3/4), 327–335.
(45) Konek, C. T.; Musorrafiti, M. J.; Al-Abadleh, H. A.; Bertin, P. A.; Nguyen, S. T.; Geiger, F. M. *J. Am. Chem. Soc.* **2004**, *126* (38), 11754–11755.
(46) Hayes, P. L.; Chen, E. H.; Achtyl, J. L.; Geiger, F. M. *J. Phys. Chem. A* **2009**, *113* (16), 4269–4280.
(47) Geiger, F. M. *Annu. Rev. Phys. Chem.* **2009**, *60*, 61–83.
(48) Malin, J. N.; Hayes, P. L.; Geiger, F. M. *J. Phys. Chem. C* **2009**, *113* (6), 2041–2052.
(49) Malin, J. N.; Holland, J. G.; Geiger, F. M. *J. Phys. Chem. C* **2009**, *113* (41), 17795–17802.
(50) Hayes, P. L.; Malin, J. N.; Konek, C. T.; Geiger, F. *Geochim. Cosmochim. Acta* **2009**, *73* (13), A506–A506.
(51) Fenter, P.; Struchio, N. C. *Prog. Surf. Sci.* **2004**, *77*, 171–258.
(52) Zohar, O.; Leizerson, I.; Sivan, U. *Phys. Rev. Lett.* **2006**, *96* (17), 177802.
(53) Fitts, J. P.; Shang, X. M.; Flynn, G. W.; Heinz, T. F.; Eisenthal, K. B. *J. Phys. Chem. B* **2005**, *109* (16), 7981–7986.
(54) Scales, P. J.; Grieser, F.; Healy, T. W.; White, L. R.; Chan, D. Y. C. *Langmuir* **1992**, *8* (3), 965–974.
(55) Larson, I.; Drummond, C. J.; Chan, D. Y. C.; Grieser, F. *Langmuir* **1997**, *13* (7), 2109–2112.
(56) Valle-Delgado, J. J.; Molina-Bolivar, J. A.; Galisteo-Gonzalez, F.; Galvez-Ruiz, M. J.; Feiler, A.; Rutland, M. W. *J. Chem. Phys.* **2005**, *123* (3), 034708.
(57) Zhang, L. N.; Singh, S.; Tian, C. S.; Shen, Y. R.; Wu, Y.; Shannon, M. A.; Brinker, C. J. *J. Chem. Phys.* **2009**, *130* (15), 154702.
(58) Ostroverkhov, V.; Waychunas, G. A.; Shen, Y. R. *Chem. Phys. Lett.* **2004**, *386* (1−3), 144–148.
(59) Ostroverkhov, V.; Waychunas, G. A.; Shen, Y. R. *Phys. Rev. Lett.* **2005**, *94* (4), 046102.

JP1037574